Polycubane Clusters: Synthesis of [Fe 4 S 4 (PR 3) 4] 1+,0 (R = Bu t , Cy, Pr i) and [Fe 4 S 4] 0 Core Aggregation upon Loss of Phosphine

ARTICLE *in* JOURNAL OF THE AMERICAN CHEMICAL SOCIETY · NOVEMBER 1996

Impact Factor: 12.11 · DOI: 10.1021/ja9620200

5 AUTHORS, INCLUDING:

Christopher Goh
Williams College
14 PUBLICATIONS **417** CITATIONS
SEE PROFILE

Brent M Segal
Harvard University
26 PUBLICATIONS **449** CITATIONS
SEE PROFILE

R. H. Holm
Harvard University
338 PUBLICATIONS **16,541** CITATIONS
SEE PROFILE

Polycubane Clusters: Synthesis of $[Fe_4S_4(PR_3)_4]^{1+,0}$ (R = Bu^t, Cy, Pr^i) and $[Fe_4S_4]^0$ Core Aggregation upon Loss of Phosphine

Christopher Goh, Brent M. Segal, Jiesheng Huang, Jeffrey R. Long, and R. H. Holm*

Contribution from the Department of Chemistry and Chemical Biology, Harvard University, Cambridge, Massachusetts 02138

Received June 17, 1996[⊗]

Abstract: The influence of tertiary phosphines on the stability of FeS_3P coordination units and the formation of iron−sulfur clusters has been investigated. Reaction of $[Fe_4S_4Cl_4]^{2-}$ with a small excess of PR_3 in acetonitrile/THF affords the cubane-type clusters $[Fe_4S_4(PR_3)_4]^{1+}$ (R = Cy, Bu^t, Pr^i), one-electron reduced over the initial cluster and possessing an $S = {}^1/_2$ ground state. These clusters may be electrochemically oxidized to $[Fe_4S_4(PR_3)_4]^{2+}$ and reduced to $[Fe_4S_4(PR_3)_4]$, which can also be generated in solution by chemical reduction. The neutral clusters upon standing in solution lose phosphine and aggregate to form *dicubane* ($[Fe_8S_8(PCy_3)_6]$) or *tetracubane* ($[Fe_{16}S_{16}(PR_3)_8]$; R = Bu^t, Pr^i) clusters. The $[Fe_8S_8]^0$ dicubane core has two intercubane Fe−S bonds, defining an Fe_2S_2 rhomb and affording a structure of overall idealized C_{2h} symmetry. The tetracubane clusters consist of a cyclic array of four cubanes joined in four Fe_2S_2 rhombs in a structure of overall D_4 symmetry, and present a new structural motif in Fe−S cluster chemistry. Tertiary phosphines impose two significant features on this cluster chemistry. These ligands significantly stabilize the $[Fe_4S_4]^{1+/0}$ core oxidation levels compared to the case of conventional $[Fe_4S_4L_4]^{3-,4-}$ clusters (L = monoanion). Ligands with cone angles exceeding that of PEt_3 (132°) favor tetrahedral FeS_3P coordination sites. This has the effect of directing reactions away from the formation of Fe_6S_6 (four trigonal pyramidal) and Fe_6S_8 (six square pyramidal) clusters having the indicated sites which are disfavored by large cone angles. Structural principles governing polycubane clusters together with a brief enumeration of stereochemically feasible polycubanes are presented and discussed.

Introduction

The synthesis of an analogue to the FeMo-cofactor of nitrogenase has posed a challenge to those hoping to gain insight into the process of dinitrogen fixation in nature. Recent disclosure of the structure of this important biological cluster,[1] whose core composition is $MoFe_7S_9$, has served both to intensify and focus that challenge. Chief among its many unanticipated structural features is the presence of six equivalent three-coordinate iron sites with the geometry shown in **3**. Although there are no known synthetic examples involving *sulfido* ligands, several compounds containing three-coordinate iron have been obtained through the use of sterically encumbered thiolate ligands.[2] In all such examples, the FeS_3 coordination environment is quite rigorously planar. This is surprisingly far from the case with the cofactor structure, wherein the iron centers are drawn in below the S_3 plane (toward the center of the cluster) by a mean distance of 0.51(6) Å.[3] For comparison, the central iron atom in a perfect FeS_4 tetrahedron with typical Fe−S distances (2.26 Å) lies 0.75 Å from the S_3 planes. Thus, the coordination geometry of the three-coordinate iron atoms in the cofactor cluster is trigonal pyramidal (or tripodal) rather than trigonal planar. In our view, the development of new strategies and reagents for accomplishing this synthetically unprecedented arrangement is an imperative step in the continuing efforts to synthesize a nitrogenase cofactor cluster analogue.

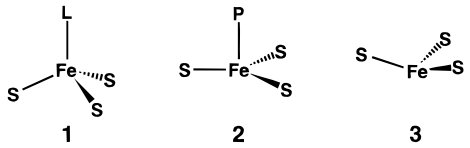

The predominant iron coordination geometry in iron−sulfur cluster chemistry is the tetrahedral arrangement depicted in **1** (L is some monodentate terminal ligand). The transformation of **1** into nitrogenase-relevant geometry **3** involves the loss of L, as well as axial translation of the Fe center down below the S_3 plane. An intermediate coordination geometry (**2**), in which the Fe atom is still four-coordinate, but has moved down into the S_3 plane, is frequently observed when L is a trialkylphosphine ligand. Examples of such behavior have been structurally elucidated in the clusters $[Fe_4S_3(NO)_4(PR_3)_3]$ (R = Et, Ph),[4] $[MFe_4S_6(PEt_3)_4X]$ (M = V, Mo; X = Cl, SPh),[5] $[Fe_6S_6(PBu^n_3)_4Cl_2]$,[6] $[Fe_6S_6(PEt_3)_4(S\text{-}p\text{-}C_6H_4Br)_2]$,[7] $[Fe_6S_6(PEt_3)_6]^{1+}$,[8] and $[Fe_7S_6(PEt_3)_4Cl_3]$.[9] Thus, the tendency for an iron site with an axial phosphine ligand to favor planar sulfur coordination over its more usual tetrahedral environment is well-documented, and might be exploited in generating reagents with some predisposition for forming clusters incorporating structural unit **3**. In particular, it is hoped that clusters with labile phosphine ligands

[⊗] Abstract published in *Advance ACS Abstracts,* November 15, 1996.

(1) (a) Chan, M. K.; Kim, J.; Rees, D. C. *Science* **1993**, *260*, 792. (b) Kim, J.; Woo, D.; Rees, D. C. *Biochemistry* **1993**, *32*, 7104.

(2) (a) Power, P. P.; Shoner, S. C. *Angew. Chem., Int. Ed. Engl.* **1991**, *30*, 330. (b) Ruhlandt-Senge, K.; Power, P. P. *Bull. Soc. Chim. Fr.* **1992**, *129*, 594. (c) MacDonnell, F. M.; Ruhlandt-Senge, K.; Ellison, J. J.; Holm, R. H.; Power, P. P. *Inorg. Chem.* **1995**, *34*, 1815.

(3) This mean distance was calculated using the latest set of crystallographic coordinates for the *Azotobacter vinelandii* MoFe protein structure; Rees, D. C., private communication.

(4) (a) Scott, M. J.; Holm, R. H. *Angew. Chem., Int. Ed. Engl.* **1993**, *32*, 564. (b) Goh, C.; Holm, R. H., unpublished results.

(5) (a) Nordlander, E.; Lee, S. C.; Cen, W.; Wu, Z. Y.; Natoli, C. R.; Di Cicco, A.; Filipponi, A.; Hedman, B.; Hodgson, K. O.; Holm, R. H. *J. Am. Chem. Soc.* **1993**, *115*, 5549. (b) Cen, W.; MacDonnell, F. M.; Scott, M. J.; Holm, R. H. *Inorg. Chem.* **1994**, *33*, 5809.

(6) (a) Synder, B. S.; Reynolds, M. S.; Noda, I.; Holm, R. H. *Inorg. Chem.* **1988**, *27*, 595. (b) Snyder, B. S.; Holm, R. H. *Inorg. Chem.* **1988**, *27*, 2339.

(7) Reynolds, M. S.; Holm, R. H. *Inorg. Chem.* **1988**, *27*, 4494.

(8) Snyder, B. S.; Holm, R. H. *Inorg. Chem.* **1990**, *29*, 274.

(9) Noda, I.; Snyder, B. S.; Holm, R. H. *Inorg. Chem.* **1986**, *25*, 3851.

S0002-7863(96)02020-3 CCC: $12.00

may be employed in directing Fe toward planar sulfur coordination, thereby initiating its collapse (with concomitant loss of phosphine) into coordination geometry **3** to ultimately yield structures approximating that of the nitrogenase cofactor.

Arguably the most pervasive structural arrangement in cluster chemistry, the cubane geometry consists of a core of four metal (M) and four nonmetal (Q) atoms distributed over alternating vertices of a cube.[10] If the metal atoms are octahedrally ligated ($M_4Q_4L_{12}$, **4**) then the cube is highly regular; however, if they are tetrahedrally ligated ($M_4Q_4L_4$, **5**) then it takes on a distorted form perhaps more aptly described as a face-capped tetrahedron. The sole example of an iron−sulfur cluster of the former type is $[Fe_4S_4(CO)_{12}]$.[11] Iron−sulfur cubane clusters of the latter

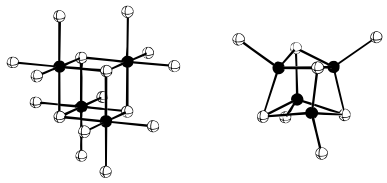

4 **5**

variety have been established as critical to the electron transfer and catalytic capabilities of numerous iron−sulfur proteins,[12] prompting considerable interest in synthetic analogue clusters of the type $[Fe_4S_4(SR)_4]^{1-,2-,3-}$.[13] This core motif has also been procured with other π-donor ligands, as in $[Fe_4S_4X_4]^{2-}$ (L = Cl^-, Br^-, I^-, HS^-, ArO^-),[14,15] with π-acceptor ligands, as in $[Fe_4S_4(NO)_4]^{1-,0}$,[16] and with an assortment of mixed ligand systems.[17,18] These last include the partially phosphine-substituted clusters $[Fe_4S_4(SPh)_2(PBu^t_3)_2]$ and $[Fe_4S_4(PBu^t_3)_3X]$ (X = Cl^-, Br^-, I^-).[18] Prior to the present work, there were no reports of either a fully phosphine-ligated iron−sulfur cubane or any clusters containing the all-ferrous cubane core $[Fe_4S_4]^0$ with geometry **5**.

In view of the preceding considerations, we have undertaken an examination of iron−sulfur cluster formation in the presence of tertiary phosphines. We seek to provide additional information on clusters accessible by phosphine terminal ligation, and on factors affecting the stabilization of tetrahedral **1** (L = PR_3) vs trigonal pyramidal **2** in such clusters. Because of the tendency of PEt_3 to effect fragment **2**,[19] we have employed tertiary phosphines with larger cone angles[20] in our synthetic systems. The work has led to the cubane clusters $[Fe_4S_4(PR_3)_4]^{1+,0}$ (R = Bu^t, Cy (cyclohexyl), Pr^i) for use in future synthetic investigations targeting a nitrogenase cofactor analogue. Moreover, the lability of the phosphine ligands on the neutral species has been found to produce a new class of polycubane aggregate clusters.

Experimental Section

Preparation of Compounds. All operations were carried out under a pure dinitrogen atmosphere using standard glovebox or Schlenk techniques. The preparation of $(Bu_4N)_2[Fe_4S_4Cl_4]$ was carried out as previously described,[14] and $(Ph_4P)_2[Fe_4S_4Cl_4]$ was produced by analogous means. $[Fe(PEt_3)_2Cl_2]$[21] was prepared via stoichiometric reaction of $FeCl_2$ and PEt_3 in THF (^{1}H NMR (C_6D_6): δ 75.8 (CH_2), 2.2 (CH_3)).

$[Fe_4S_4(PBu^t_3)_4](BPh_4)\cdot 2MeCN$. A solution of tri-*tert*-butylphosphine (588 mg, 2.91 mmol) in 20 mL of THF was added to a stirred solution of $(Bu_4N)_2[Fe_4S_4Cl_4]$ (630 mg, 0.664 mmol) in 20 mL of acetonitrile, inducing an immediate color change from red-brown to brown. Solid $Na(BPh_4)$ (884 mg, 2.58 mmol) was added to the solution, which, after 1 h of stirring, was filtered and its volume reduced in vacuo to *ca*. 10 mL. The brown-black block-shaped crystals that formed were collected by filtration and washed with small aliquots of acetonitrile to give 680 mg (70%) of product. ^{1}H NMR (CD_2Cl_2): δ 7.31 (m), 7.03 (m), 6.88 (t), 2.75 (CH_3). FAB-MS (*m*/*z*): 1160 (M^+), 958 ($M^+ - PBu^t_3$), 756 ($M^+ - 2PBu^t_3$), 554 ($M^+ - 3PBu^t_3$), 352 ($M^+ - 4PBu^t_3$). Absorption spectrum (CH_2Cl_2): λ_{max} (ϵ_M) 269 (sh, 28900), 298 (sh, 22800) nm. μ_{eff} = 4.19 μ_B (297 K). An analytical sample was recrystallized from dichloromethane. Anal. Calcd for $C_{74}H_{132}BCl_4Fe_4P_4S_4$: C, 53.87; H, 8.06; B, 0.66; Cl, 8.59; Fe, 13.54; P, 7.51; S, 7.77. Found: C, 53.56; H, 7.76; B, 0.63; Cl, 6.41; Fe, 13.58; P, 7.44; S, 7.78.

$[Fe_4S_4(PCy_3)_4](BPh_4)$. A solution of tricyclohexylphosphine (525 mg, 1.87 mmol) in 20 mL of THF was added to a stirred suspension of $(Ph_4P)_2[Fe_4S_4Cl_4]$ (500 mg, 0.427 mmol) in 10 mL of acetonitrile. After 15 min, a dark brown solution had formed; a solution of $Na(BPh_4)$ (600 mg, 1.75 mmol) in 10 mL of acetonitrile was added, producing an immediate gray precipitate (NaCl and $(Ph_4P)(BPh_4)$). The mixture was stirred for 2 h and filtered through Celite, and the filtrate was reduced to dryness under vacuum. The dark brown residue was washed with acetonitrile and ether (3 × 15 mL each), and redissolved in 15 mL of THF. The solution was filtered (removing a small amount of gray solid), layered with 30 mL of ether, and stored overnight at −20 °C to afford 480 mg (63%) of product as brown-black block-shaped crystals. ^{1}H NMR (CD_2Cl_2): δ 7.31 (m), 7.03 (m), 6.88 (t), 4.78 (P−CH), 2.50−1.25 (m, CH_2). FAB-MS (*m*/*z*): 1472 (M^+), 1192 ($M^+ - PCy_3$), 912 ($M^+ - 2PCy_3$), 632 ($M^+ - 3PCy_3$), 352 ($M^+ - 4PCy_3$). μ_{eff} = 3.43 μ_B (296 K). Anal. Calcd for $C_{96}H_{152}BFe_4P_4S_4$: C, 64.32; H, 8.55; B, 0.60; Fe, 12.46; P, 6.91; S, 7.15. Found: C, 64.28; H, 8.43; B, 0.57; Fe, 12.58; P, 7.08; S, 7.14.

$[Fe_4S_4(PPr^i_3)_4](BPh_4)$. This preparation was analogous to that of $[Fe_4S_4(PCy_3)_4](BPh_4)$, using 0.85 mmol of initial cluster and 3.75 mmol of tri-*iso*-propylphosphine in 40 mL of acetonitrile. The product was isolated as 740 mg (66%) of black elongated rhombohedral crystals. ^{1}H NMR ($CDCl_3$): δ 7.46 (m), 7.09 (m), 6.93 (t), 4.82 (P−CH), 2.30 (CH_3). FAB-MS (*m*/*z*): 992 (M^+), 832 ($M^+ - PPr^i_3$), 672 ($M^+ - 2PPr^i_3$), 512 ($M^+ - 3PPr^i_3$), 352 ($M^+ - 4PPr^i_3$). This compound was further identified by a single-crystal X-ray structure determination.

$[Fe_4S_4(PR_3)_4]$. Neutral clusters were generated by reduction of the preceding cluster cations. Despite multiple attempts, they could not be isolated in pure crystalline form. **(a) $[Fe_4S_4(PBu^t_3)_4]$.** A solution of freshly generated sodium acenaphthalenide (14 mg, 81 μmol) in 10 mL of THF was added dropwise to a stirred solution of $[Fe_4S_4(PBu^t_3)_4](BPh_4)$ (110 mg, 73 μmol) in 10 mL of THF maintained at −78 °C. The residue was extracted into benzene to give a brown-black solution of the product. FAB-MS (*m*/*z*): 1160 (M^+), 958 ($M^+ - PBu^t_3$), 756 ($M^+ - 2PBu^t_3$), 554 ($M^+ - 3PBu^t_3$), 352 ($M^+ - 4PBu^t_3$).

(10) This arrangement is sometimes referred to as a heterocubane geometry to distinguish it from structures in which all eight cube vertices are identical, as in the original hydrocarbon cubane, C_8H_8: Eaton, P. E.; Cole, T. W., Jr. *J. Am. Chem. Soc*. **1964**, *86*, 3158.

(11) Nelson, L. L.; Lo, F. Y.-K.; Rae, A. D.; Dahl, L. F. *J. Organomet. Chem*. **1982**, *225*, 309.

(12) (a) *Iron−Sulfur Proteins*; Spiro, T. G., Ed.; Wiley-Interscience: New York, 1982. (b) Cammack, R. *Adv. Inorg. Chem*. **1992**, *38*, 281.

(13) (a) Berg, J. M.; Holm, R. H. In *Iron−Sulfur Proteins*; Spiro, T. G., Ed.; Wiley-Interscience: New York, 1982, Chapter 1. (b) Carney, M. J.; Papaefthymiou, G. C.; Spartalian, K.; Frankel, R. B.; Holm, R. H. *J. Am. Chem. Soc*. **1988**, *110*, 6084 and references therein. (c) O'Sullivan, T.; Millar, M. M. *J. Am. Chem. Soc*. **1985**, *107*, 4096.

(14) Wong, G. B.; Bobrik, M. A.; Holm, R. H. *Inorg. Chem*. **1978**, *17*, 578.

(15) (a) Müller, A.; Schladerbeck, N. H.; Bögge, H. *J. Chem. Soc., Chem. Commun*. **1987**, *35*. (b) Cleland, W. E.; Holtman, D. A.; Sabat, M.; Ibers, J. A.; DeFotis, G. C.; Averill, B. A. *J. Am. Chem. Soc*. **1983**, *105*, 6021.

(16) Chu, C. T.-W.; Lo, F. Y.-K.; Dahl, L. F. *J. Am. Chem. Soc*. **1982**, *104*, 3409.

(17) (a) Stack, T. D. P.; Weigel, J. A.; Holm, R. H. *Inorg. Chem*. **1990**, *29*, 3745. (b) Holm, R. H.; Ciurli, S.; Weigel, J. A. *Prog. Inorg. Chem*. **1990**, *38*, 1.

(18) Tyson, M. A.; Demadis, K. D.; Coucouvanis, D. *Inorg. Chem*. **1995**, *34*, 4519.

(19) $FeS_3(PEt_3)$ sites more closely approaching **1** than **2** occur in $[Fe_6S_6(PEt_3)_6]^{1+}$ (2 sites)[8] and $[Fe_7S_6(PEt_3)_4Cl_3]$ (1 site).[9]

(20) Tolman, C. A. *Chem. Rev*. **1975**, *77*, 313. The following cone angles of PR_3 ligands are pertinent to this work: R = Et (132°), Ph (145°), Pr^i (160°), Cy (170°), Bu^t (182°).

(21) Booth, G.; Chatt, J. *J. Chem. Soc*. **1962**, 2009.

Table 1. Crystallographic Data[a] for $[Fe_4S_4(PBu^t_3)_4](BPh_4)\cdot 2MeCN$, $[Fe_4S_4(PCy_3)_4](BPh_4)$, and $[Fe_4S_4(PPr^i_3)_4](BPh_4)$

	$[Fe_4S_4(PBu^t_3)_4](BPh_4)\cdot 2MeCN$	$[Fe_4S_4(PCy_3)_4](BPh_4)$	$[Fe_4S_4(PPr^i_3)_4](BPh_4)$
formula	$C_{76}H_{134}BFe_4N_2P_4S_4$	$C_{96}H_{152}BFe_4P_4S_4$	$C_{60}H_{104}BFe_4P_4S_4$
formula wt	1562.27	1792.64	1311.76
T, K	213	223	213
crystal system	monoclinic	monoclinic	monoclinic
space group	$P2_1/c$	$P2_1/c$	$P2_1/c$
Z	4	4	4
a, Å	14.514(3)	14.909(3)	17.9899(2)
b, Å	20.555(4)	21.400(5)	17.3893(2)
c, Å	28.535(5)	30.322(5)	23.1191(1)
β, deg	99.37(1)	94.52(2)	108.483(1)
V, Å^3	8399(3)	9644(3)	6859.3(1)
d_{calc}, g/cm^3	1.233	1.232	1.270
*wR*2,[b] *R*1[c]	0.0902, 0.0554	0.1239, 0.0650	0.1043, 0.0457

[a] Obtained with graphite monochromated Mo Kα ($\lambda = 0.71073$ Å) radiation. [b] $wR2 = \{\sum[w(F_o^2 - F_c^2)^2]/\sum[w(F_o^2)^2]\}^{1/2}$. [c] $R1 = \sum||F_o| - F_c||/\sum|F_o|$.

Table 2. Crystallographic Data[a] for $[Fe_{16}S_{16}(PBu^t_3)_8]\cdot 2C_6H_{14}\cdot C_6H_6$, $[Fe_{16}S_{16}(PPr^i_3)_8]\cdot 2MeCN$, and $[Fe_8S_6Cl_4(PCy_3)_4]\cdot 3THF$

	$[Fe_{16}S_{16}(PBu^t_3)_8]\cdot 2C_6H_{14}\cdot C_6H_6$	$[Fe_{16}S_{16}(PPr^i_3)_8]\cdot 2MeCN$	$[Fe_8S_6Cl_4(PCy_3)_4]\cdot 3THF$
formula	$C_{114}H_{250}Fe_{16}P_8S_{16}$	$C_{76}H_{174}Fe_{16}N_2P_8S_{16}$	$C_{84}H_{156}Cl_4Fe_8O_3P_4S_6$
formula wt	3275.57	2770.49	2118.93
T, K	213	223	223
crystal system	tetragonal	orthorhombic	tetragonal
space group	*P*4/*ncc*	*Pbcn*	$I\bar{4}$
Z	4	4	2
a, Å	25.1860(4)	15.865(6)	16.826(8)
b, Å		31.059(12)	
c, Å	26.2846(6)	25.095(11)	18.126(9)
V, Å^3	16673.2(5)	12366(9)	5132(4)
d_{calc}, g/cm^3	1.282	1.488	1.371
*wR*2, *R*1[b]	0.1573, 0.0646	0.1576, 0.0690	0.1808, 0.0696

[a] Obtained with graphite monochromated Mo Kα ($\lambda = 0.71073$ Å) radiation. [b] For definitions *cf.* Table 1.

(b) $[Fe_4S_4(PCy_3)_4]$. A solution of freshly generated sodium acenaphthalenide (40 mg, 230 μmol) in 10 mL of THF was added dropwise to a stirred solution of $[Fe_4S_4(PCy_3)_4](BPh_4)$ (364 mg, 200 μmol) in 20 mL of THF maintained at −78 °C. The solution changed color from dark brown to purple-black, and was reduced to dryness under vacuum. The residue was extracted into toluene to give a brown-black solution of the product. FAB-MS (*m*/*z*): 1472 (M^+), 1192 ($M^+ - PCy_3$), 912 ($M^+ - 2PCy_3$), 632 ($M^+ - 3PCy_3$), 352 ($M^+ - 4PCy_3$).

(c) $[Fe_4S_4(PPr^i_3)_4]$. A solution of freshly generated sodium acenaphthalenide (24.5 mg, 140 μmol) in 10 mL of THF was added dropwise to a stirred solution of $[Fe_4S_4(PPr^i_3)_4](BPh_4)$ (167 mg, 127 μmol) in 10 mL of THF maintained at −78 °C. The residue was extracted into benzene to give a brown-black solution of the product. FAB-MS (*m*/*z*): 992 (M^+), 832 ($M^+ - PPr^i_3$), 672 ($M^+ - 2PPr^i_3$), 512 ($M^+ - 3PPr^i_3$), 352 ($M^+ - 4PPr^i_3$).

$[Fe_8S_8(PCy_3)_6]\cdot C_7H_8$. This preparation is a slightly refined version of one reported previously.[22] A mixture of $[Fe(PEt_3)_2Cl_2]$ (5.0 g, 14 mmol) and NaSPh (3.6 g, 27 mmol) was stirred in 50 mL of toluene for 2 h to give a deep red solution over a white solid. The solution was filtered through Celite twice, and dibenzyl trisulfide (5.8 g, 21 mmol) was added, inducing an immediate color change to dark brown and precipitation of a small amount of black solid. After the mixture was stirred for 20 min, tricyclohexylphosphine (10 g, 36 mmol) was added, and the solution was filtered, concentrated to 20 mL under reduced pressure, and allowed to stand for up to 6 days. The product (1.8 g, 42%) was recovered in the form of black rhombic plates. $\mu_{eff} = 6.80\ \mu_B$ (296 K). Anal. Calcd for $C_{115}H_{206}Fe_8P_6S_8$: C, 55.74; H, 8.38; Fe, 18.03; P, 7.50; S, 10.35. Found: C, 55.93; H, 8.19; Fe, 18.16; P, 7.29; S, 10.50. This compound is virtually insoluble in all common organic solvents.

$[Fe_{16}S_{16}(PBu^t_3)_8]\cdot 2C_6H_{14}\cdot C_6H_6$. A benzene solution of $[Fe_4S_4(PBu^t_3)_4]$ (prepared as described above) was layered with hexane. After 3 days, black block-shaped crystals of $[Fe_{16}S_{16}(PBu^t_3)_8]\cdot 2C_6H_{14}\cdot C_6H_6$ had formed. The crystals were collected, washed with hexane, and dried *in vacuo* to give 230 mg (27%) of product. This compound was identified by a single-crystal X-ray structure determination (and by matching single-crystal unit cell parameters in subsequent preparations) and is virtually insoluble in all common organic solvents.

$[Fe_{16}S_{16}(PPr^i_3)_8]\cdot 2MeCN$. A mixture of $[Fe(PEt_3)_2Cl_2]$ (1.0 g, 2.7 mmol) and NaSPh (720 mg, 5.4 mmol) was stirred in 20 mL of toluene for 2 h to give a deep red solution over a white solid. The solution was filtered through Celite twice, and benzyl trisulfide (1.2 g, 4.3 mmol) was added, inducing an immediate color change to dark brown and precipitation of a small amount of black solid. After the mixture was stirred for 20 min, tri-*iso*-propylphosphine (1.0 g, 6.2 mmol) was added, and the resulting mixture was reduced to dryness under vacuum. The resulting black residue was redissolved in 20 mL of acetonitrile; this solution was filtered, allowed to stand for 4 days, and concentrated to *ca*. 15 mL under reduced pressure. Upon decanting the colorless supernatant liquid, a dark crystalline solid immersed in a thick black oil was obtained. The oil was removed by repeated washings with ether and hexane to give a black solid, primarily in the form of rhombic plate crystals. This preparation was repeated several times, with variable but low yields of no more than 85 mg (18%). The compound was identified by a single-crystal X-ray structure determination, and is virtually insoluble in all common organic solvents.

$[Fe_8S_6Cl_4(PCy_3)_4]$. Solid $[Fe_8S_8(PCy_3)_6]\cdot C_7H_8$ (320 mg, 129 μmol) was added to 20 mL of chloroform and stirred for 2 h to give a dark brown solution. The solution was reduced to dryness under vacuum, and the dark brown residue was redissolved in THF. This solution was filtered and layered with hexane. After several days, black rhombohedral crystals of $[Fe_8S_6Cl_4(PCy_3)_4]\cdot 3THF$ (identified by a single-crystal X-ray structure determination) had formed; the crystals were collected, washed with hexane, and dried *in vacuo* to give 45 mg (17%) of product.

X-ray Structure Determinations. Structures were determined for the six compounds listed in Tables 1 and 2. Single crystals were picked from the reaction products, coated with Apiezon L grease, and attached to glass fibers. The crystals were then transferred to a Siemens SMART ($[Fe_4S_4(PPr^i_3)_4](BPh_4)$ and $[Fe_{16}S_{16}(PBu^t_3)_8]\cdot 2C_6H_{14}\cdot C_6H_6$) or a Nicolet P3 (all others) diffractometer and cooled in a dinitrogen stream. Lattice parameters were obtained from a least-squares analysis of more than

(22) Cai, L.; Segal, B. M.; Long, J. R.; Scott, M. J.; Holm, R. H. *J. Am. Chem. Soc.* **1995**, *117*, 8863.

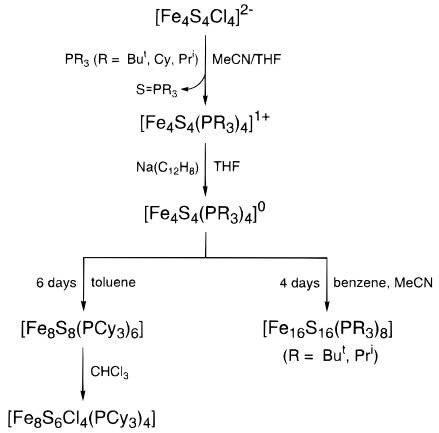

Figure 1. Synthesis and reactivity of phosphine-ligated mono-, di-, and tetracubane clusters.

30 carefully centered reflections. None of the crystals showed significant decay during data collection. The raw intensity data were converted (including corrections for scan speed, background, and Lorentz and polarization effects) to structure factor amplitudes and their esd's. An empirical absorption correction based on the observed variation in intensity of azimuthal (Ψ) scans was applied to each data set.

Space group assignments were based on systematic absences, *E* statistics, and successful refinement of the structures. Structures were solved by direct methods with the aid of successive difference Fourier maps, and refined against all data using the SHELXTL 5.0 software package. Thermal parameters for all non-hydrogen atoms were refined anisotropically. Hydrogen atoms were assigned to ideal positions and refined using a riding model with an isotropic thermal parameter 1.2 times that of the attached carbon atom (1.5 times for methyl hydrogens). The hexane and benzene solvate molecules in the structure of $[Fe_{16}S_{16}(PBu^t_3)_8]\cdot 2C_6H_{14}\cdot C_6H_6$ are each disordered over two positions. One of the THF solvate molecules in the structure of $[Fe_8S_6Cl_4(PCy_3)_4]\cdot 3THF$ is severely disordered; its atoms could not be distinguished as carbon or oxygen. Hydrogen atoms were not included for these disordered solvate molecules. Crystallographic data are listed in Tables 1 and 2. Further details of the structure determinations are deposited as Supporting Information.[23]

Other Physical Measurements. Absorption spectra were measured with a Cary Model 3 spectrophotometer. FAB mass spectrometric measurements were made on a JEOL SX-102 instrument. Cyclic voltammetry was performed with an EG&G Model 163 potentiostat, 0.1 M $(Bu_4N)(PF_6)$ supporting electrolyte, and a Pt disk working electrode. Potentials were determined vs an SCE reference electrode. EPR spectra were recorded at 15 K on a Bruker ESP 300-E spectrometer operating at X-band frequencies and employing a Bruker ER 412VT-E10 liquid nitrogen variable-temperature apparatus. Mössbauer spectroscopic data were collected (at 77 K) and analyzed with equipment and procedures described elsewhere.[2c] Isomer shifts are referenced to Fe metal at room temperature. Magnetic susceptibilities were determined using a Johnson Matthey magnetic susceptibility balance.

Results and Discussion

Monocubane Clusters. Preparations of the phosphine-ligated monocubane clusters are summarized, along with other cluster preparations, in the reaction scheme of Figure 1.

(a) $[Fe_4S_4(PR_3)_4]^{1+}$ (R = Bu^t, Cy, Pr^i). The synthesis of the $[Fe_4S_4(PR_3)_4]^{1+}$ (R = Bu^t, Cy, Pr^i) cubane clusters is achieved by direct reaction of $[Fe_4S_4Cl_4]^{2-}$ with a slight excess of PR_3. In these reactions, the phosphine serves as both a ligand and a reducing agent; the use of additional phosphine did not improve product yields. Trialkylphosphine sulfide was identified in the mass spectrum of the reaction mixtures, and was separated from the products by washing with acetonitrile. A similar reaction using slightly less phosphine is reported to yield the partially substituted cubane $[Fe_4S_4(PBu^t)_3Cl]$.[18]

(23) See paragraph at the end of this article concerning Supporting Information.

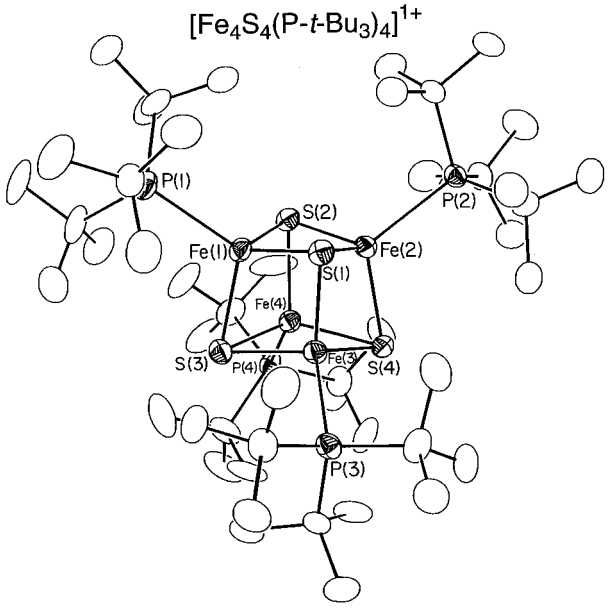

Figure 2. Structure (50% probability ellipsoids) and atom labeling scheme of the cubane cluster $[Fe_4S_4(PBu^t_3)_4]^{1+}$; hydrogen atoms are omitted for clarity.

The structures of $[Fe_4S_4(PBu^t_3)_4](BPh_4)\cdot 2MeCN$, $[Fe_4S_4(PCy_3)_4](BPh_4)$, and $[Fe_4S_4(PPr^i_3)_4](BPh_4)$ were determined by single-crystal X-ray analyses. Because of nearly identical structures, only the structure of $[Fe_4S_4(PBu^t_3)_4]^{1+}$, depicted in Figure 2, is described. It consists of the standard face-capped tetrahedral cubane geometry (**5**) with four terminal PBu^t_3 ligands. Selected interatomic distances and angles are listed in Table 3. The $[Fe_4S_4]^{1+}$ cluster core closely approaches its ideal T_d symmetry, and exhibits mean bond distances (Fe−Fe 2.75(1) Å, Fe−S 2.28(1) Å, and Fe−P 2.458(9) Å) that compare favorably with those of $[Fe_4S_4(PBu^t)_3Cl]$.[18] Although lacking here and in $[Fe_4S_4(PPr^i_3)_4]^{1+}$, the previously recognized "plasticity" of the $[Fe_4S_4]^{1+}$ core (apparently due to exogenous packing forces)[13b] is evident in the structure of $[Fe_4S_4(PCy_3)_4]^{1+}$, which displays some variation in its Fe−S bond lengths over the range 2.222(2)−2.305(3) Å. The mean Fe−P distances in the set $[Fe_4S_4(PR_3)_4]^{1+}$, 2.39(6) Å (R = Pr^i), 2.40(3) Å (R = Cy), 2.459(9)) Å (R = Bu^t), roughly correlate with differences in phosphine ligand cone angle.[20]

The clusters $[Fe_4S_4(PR_3)_4]^{1+}$ were further characterized spectroscopically. The Mössbauer spectrum of $[Fe_4S_4(PBu^t_3)_4]^{1+}$, shown in Figure 3, consists of a single symmetric quadrupole doublet. Isomer shifts for three cationic clusters are contained in Table 4. Their values (0.46−0.51 mm/s) tend to fall just below the usual range for $[Fe_4S_4(SR)_4]^{3-}$ clusters (0.52−0.62 mm/s),[13b,24] indicating that the change of terminal ligand, phosphine for thiolate, produces a small but noticeable decrease in isomer shifts. On the other hand, the shifts for $[Fe_6S_6(PEt_3)_6]^{1+}$ (0.50−0.53 mm/s[8]), whose mean oxidation state ($Fe^{2.17+}$) is practically the same as that of the clusters, are in rather good agreement with those of $[Fe_4S_4(PR_3)_4]^{1+}$. The axial EPR spectra of $[Fe_4S_4(PBu^t_3)_4]^{1+}$ and $[Fe_4S_4(PCy_3)_4]^{1+}$ in frozen solutions, presented in Figure 4, are indicative of an $S = {}^1/_2$ ground state. They differ from those of reduced iron−sulfur proteins and $[Fe_4S_4(SR)_4]^{3-}$ clusters ($g_\perp \sim 2.05$, $g_\parallel \sim 1.93$)[24ab] in their larger anisotropies, such that $g_{av} = 2.00$ rather than $g_{av} < 2$. These spectra also resemble the rhombic spectrum of $[Fe_4S_4(PBu^t_3)_3Cl]$ ($g \approx 2.12, 1.95, 1.91$).[18] The structural and

Table 3. Selected Interatomic Distances (Å) and Angles (deg) for $[Fe_4S_4(PBu^t_3)_4]^{1+}$

Fe(1)−S(1)	2.288(2)	Fe(1)−P(1)	2.461(2)
Fe(1)−S(2)	2.282(2)	Fe(2)−P(2)	2.459(2)
Fe(1)−S(3)	2.265(2)	Fe(3)−P(3)	2.443(2)
Fe(2)−S(1)	2.287(2)	Fe(4)−P(4)	2.468(2)
Fe(2)−S(2)	2.285(2)	mean of 4	2.458(9)
Fe(2)−S(4)	2.278(2)		
Fe(3)−S(1)	2.261(2)		
Fe(3)−S(3)	2.281(2)		
Fe(3)−S(4)	2.289(2)	S(2)−Fe(1)−S(1)	104.30(8)
Fe(4)−S(2)	2.269(2)	S(3)−Fe(1)−S(1)	103.62(8)
Fe(4)−S(3)	2.279(2)	S(3)−Fe(1)−S(2)	103.38(8)
Fe(4)−S(4)	2.304(2)	S(2)−Fe(2)−S(1)	104.24(8)
mean of 12	2.28(1)	S(4)−Fe(2)−S(2)	103.57(8)
		S(4)−Fe(2)−S(1)	103.68(8)
Fe(1)−Fe(2)	2.749(2)	S(1)−Fe(3)−S(3)	104.00(8)
Fe(1)−Fe(3)	2.740(2)	S(1)−Fe(3)−S(4)	104.18(8)
Fe(1)−Fe(4)	2.757(2)	S(3)−Fe(3)−S(4)	104.12(8)
Fe(2)−Fe(3)	2.740(2)	S(2)−Fe(4)−S(3)	103.36(8)
Fe(2)−Fe(4)	2.766(2)	S(2)−Fe(4)−S(4)	103.24(8)
Fe(3)−Fe(4)	2.761(2)	S(3)−Fe(4)−S(4)	103.70(8)
mean of 6	2.75(1)	mean of 12	103.8(4)
S(1)−Fe(1)−P(1)	115.68(8)	Fe(2)−S(1)−Fe(1)	73.84(7)
S(2)−Fe(1)−P(1)	114.14(9)	Fe(3)−S(1)−Fe(1)	74.08(7)
S(3)−Fe(1)−P(1)	114.29(8)	Fe(3)−S(1)−Fe(2)	74.09(7)
S(1)−Fe(2)−P(2)	113.83(8)	Fe(1)−S(2)−Fe(2)	74.00(7)
S(2)−Fe(2)−P(2)	113.46(8)	Fe(4)−S(2)−Fe(1)	74.58(7)
S(4)−Fe(2)−P(2)	116.67(8)	Fe(4)−S(2)−Fe(2)	74.80(7)
S(1)−Fe(3)−P(3)	115.14(8)	Fe(1)−S(3)−Fe(3)	74.13(7)
S(3)−Fe(3)−P(3)	112.03(8)	Fe(1)−S(3)−Fe(4)	74.72(7)
S(4)−Fe(3)−P(3)	116.06(8)	Fe(4)−S(3)−Fe(3)	74.52(7)
S(2)−Fe(4)−P(4)	116.92(8)	Fe(2)−S(4)−Fe(3)	73.74(7)
S(3)−Fe(4)−P(4)	112.90(8)	Fe(2)−S(4)−Fe(4)	74.27(7)
S(4)−Fe(4)−P(4)	115.12(8)	Fe(3)−S(4)−Fe(4)	73.90(7)
mean of 12	115(1)	mean of 12	74.2(3)

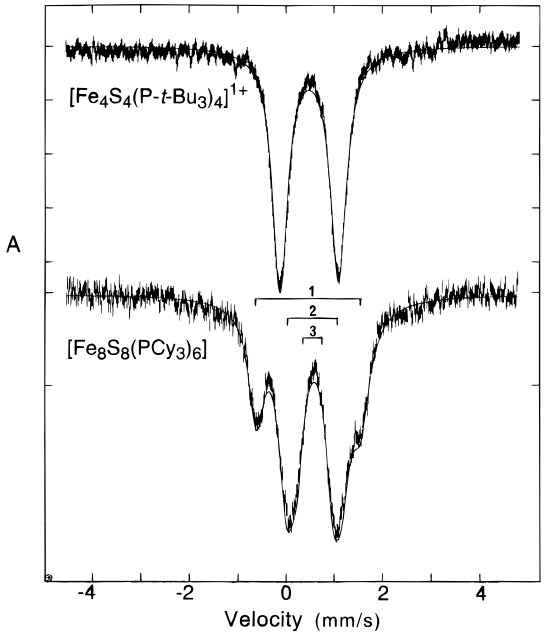

Figure 3. Zero-field Mössbauer spectra of $[Fe_4S_4(PBu^t_3)_4](BPh_4)$ (top) and $[Fe_8S_8(PCy_3)_6]$ (bottom) at 77 K.

spectroscopic results clearly establish the cubane-type $[Fe_4S_4]^{1+}$ core with $S = {}^1/_2$ and the mean oxidation state $Fe^{2.25+}$.

(b) $[Fe_4S_4(PR_3)_4]$ (R = Bu^t, Cy, Pr^i). The cyclic voltammogram of $[Fe_4S_4(PBu^t_3)_4]^{1+}$ in dichloromethane, set out in Figure 5, reveals chemically reversible ($i_{pa}/i_{pc} \approx 1$) oxidation and reduction steps at $E_{1/2} = 0.16$ and -0.98 V, respectively. The cyclic voltammograms of other $[Fe_4S_4(PR_3)_4]^{1+}$ clusters in dichloromethane differ unimportantly, with $E_{1/2} = 0.13$ and -1.06 V (R = Cy) and 0.16 and -0.99 V (R = Pr^i).

Table 4. Mössbauer Parameters of $[Fe_4S_4(PR_3)_4](BPh_4)$ and $[Fe_8S_8(PCy_3)_6]$[a]

	mm/s	
cluster	δ[b]	ΔE_Q
R = Pr^i	0.46	1.06
R = Cy	0.48	1.23
R = Bu^t	0.51	0.77
$[Fe_8S_8(PCy_3)_6]$	0.49[c]	2.20
	0.60[d]	1.14
	0.62[e]	0.73

[a] All measurements at 77 K. [b] Relative to Fe metal at room temperature. [c] 27%. [d] 47%. [e] 21%.

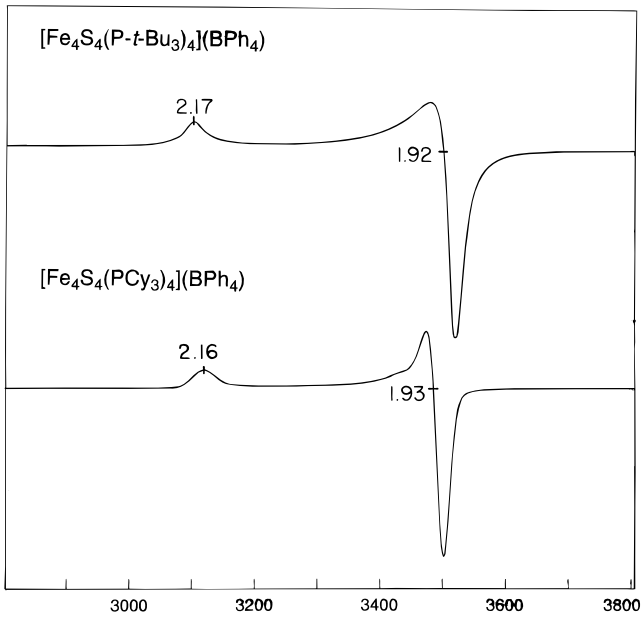

Figure 4. EPR spectra of $[Fe_4S_4(PBu^t_3)_4](BPh_4)\cdot 2MeCN$ (top) and $[Fe_4S_4(PCy_3)_4](BPh_4)$ (bottom) in frozen dichloromethane at 15 K.

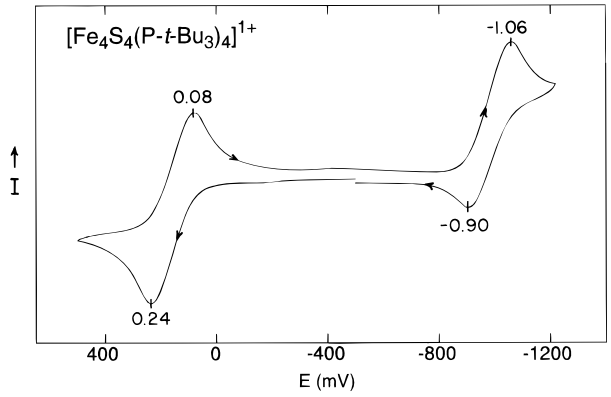

Figure 5. Cyclic voltammogram of $[Fe_4S_4(PBu^t_3)_4](BPh_4)\cdot 2MeCN$ in dichloromethane at 298 K.

Consequently, these clusters form the three-member electron transfer series $[Fe_4S_4(PR_3)_4]^{2+,1+,0}$. Attempts at preparing the clusters $[Fe_4S_4(PR_3)_4]^{2+}$ (R = Bu^t, Cy) by chemical oxidation with $(Cp_2Fe)^+$, Ag^+, or I_2 were not demonstrably successful. In contrast, the reduced clusters $[Fe_4S_4(PR_3)_4]$ (R = Bu^t, Cy, Pr^i) are easily realized by reaction of $[Fe_4S_4(PR_3)_4]^{1+}$ with slightly more than 1 equiv of sodium acenaphthalenide. Unlike their monopositive precursors, the neutral black cubane clusters are soluble in benzene and toluene, enabling their unequivocal identification by mass spectrometry. The results for $[Fe_4S_4(PBu^t_3)_4]$, provided in Figure 6, are typical. The molecular parent ion with the correct isotope distribution is observed (*m*/*z* 1160). A set of four peaks separated by *m*/*z* 202 corresponds

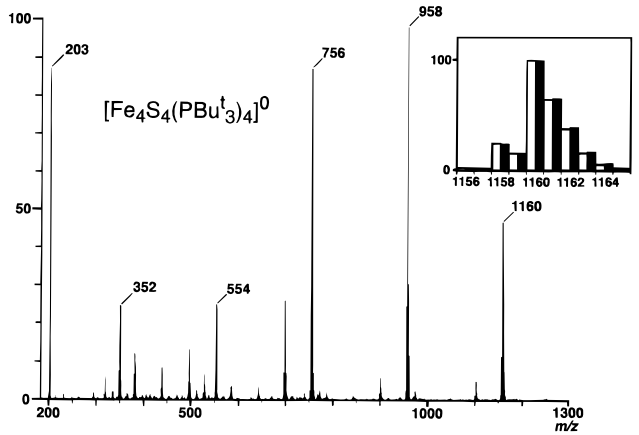

Figure 6. Positive ion FAB mass spectrum of $[Fe_4S_4(PBu^t_3)_4]$. The inlay displays the observed (white) and theoretical (black) isotope distributions for the parent ion mass. Numerically labeled peaks correspond to PBu^t_3 and $[Fe_4S_4(PBu^t_3)_p]$ ($p = 0-4$) from left to right, respectively.

to sequential loss of PBu^t_3, until $Fe_4S_4^{1+}$ observed at *m*/*z* 352. However, owing to the apparent lability of the phosphine ligands, the neutral cluster species could not be isolated in pure solid form despite multiple attempts.

From the foregoing results and additional observations, we conclude that (i) tertiary phosphines are more effective than other ligands in stabilizing reduced $[Fe_4S_4]^{1+,0}$ cores in type **5** clusters and (ii) the cone angle of the phosphine contributes to the structure formed. While extremely prone to oxidation, the clusters $[Fe_4S_4(SR)_4]^{3-}$ are nonetheless prepared and manipulated without difficulty.[13b,24] Although readily formed as $[Fe_4S_4(PR_3)_4]$ with bulky phosphines, the $[Fe_4S_4]^0$ core has never been isolated, and rarely detected *in situ*,[25,26] in conventional $[Fe_4S_4X_4]^{4-}$ clusters were X is a monoanionic ligand. For example, in the redox series $[Fe_4S_4(SPh)_4]^z$ in acetonitrile, the potentials -1.00 V ($z = 2-/3-$) and -1.72 V ($z = 3-/4-$) are 1.16 and 0.74 V more negative, respectively, than the corresponding values in Figure 5. These very large positive potential shifts arise from two inseparable features: the tendency of tertiary phosphines to stabilize lower oxidation states and the much reduced negative charges of the cluster molecules.

With regard to (ii), we summarize certain observations. Reaction of 1 equiv of $[Fe_4S_4Cl_4]^{2-}$ with 2 equiv of $[FeCl_2(PEt_3)_2]$ in acetonitrile affords the basket cluster $[Fe_6S_6(PEt_3)_4Cl_2]$ (70%, $Fe^{2.33+}$).[6b] Further, reaction of $[Fe(OH_2)_6]^{2+}$ with 1 equiv of Li_2S and excess PEt_3 in THF produces the fully substituted basket cluster $[Fe_6S_6(PEt_3)_6]^{1+}$ (14%, $Fe^{2.17+}$) as the only isolable product.[8] Both clusters are prepared under anaerobic conditions; in terms of mean iron oxidation state, the products are more reduced than the starting cluster. Further, both contain two type-**1** and four type-**2** sites; the latter will suffer steric strain and possibly induce cluster instability if phosphines with larger cone angles were to be included. Reactions of Fe(II) with excess PEt_3 under oxidizing conditions lead to the formation of $[Fe_6S_8(PEt_6)_6]^{2+,1+}$ in low isolated yields (*ca*. 15%).[27,28] These face-capped octahedral clusters feature square-pyramidal FeS_4P coordination units with the iron atom *ca*. 0.25−0.30 Å above the S_4 plane in the direction of the axial phosphorus atom. While the phosphine sustains the mean oxidation states $Fe^{3+,2.83+}$ in these clusters (abetted by *four* μ_3-S atoms), the coordination unit would also be strained by large phosphines. Because of the much larger displacement of the iron atom from the S_3 plane, the FeS_3L site **1** at parity of L = PR_3 is subjected to less steric overextension than site **2**. In addition to the existence of $[Fe_4S_4(PR_3)_4]^{1+,0}$ (R = Cy, Pr^i, Bu^t), this point is supported by the synthesis of the cubane-type clusters $[Co_4Q_4(PBu^t_3)_4]$ (Q = S, Se)[29] and $[Fe_4Te_4(PPr^i_3)_4]$.[30] We do not claim that the species $[Fe_4S_4(PEt_3)_4]^{1+,0}$ are incapable of existence,[31] but only that they may be precursors of other, more stable, clusters. In Fe−S−PEt_3 systems, we have come to recognize Fe_6S_6 and Fe_6S_8 clusters as byproduct "sinks" when endeavoring to prepare other types of clusters. Elsewhere, the influence of cone angle on cluster structure has been noted.[18,30]

Dicubane Cluster: $[Fe_8S_8(PCy_3)_6]$. As indicated in the reaction scheme of Figure 1, the neutral clusters $[Fe_4S_4(PR_3)_4]$ (R = Bu^t, Cy, Pr^i), upon standing in solution at room temperature for several days, lose some of their phosphine ligands and aggregate to form insoluble di- or tetracubane clusters. When R = Cy, the dicubane cluster $[Fe_8S_8(PCy_3)_6]$ is formed. However, the most efficient route to its preparation is not the one delineated in the scheme of Figure 1, but rather involves direct self-assembly of the neutral cubane precursor $[Fe_4S_4(PCy_3)_4]$ in toluene (identified by its positive ion FAB mass spectrum) from $[Fe(PEt_3)_2Cl_2]$, NaSPh, $PhCH_2SSSCH_2$-Ph, and PCy_3. After standing for up to 6 days, this solution produces black rhombic plate crystals of $[Fe_8S_8(PCy_3)_6]\cdot C_7H_8$ in *ca*. 40% overall yield. The product was identified by an X-ray structure determination.

The core structure of the dicubane cluster, as obtained from one of these crystals,[22] is depicted in Figure 7. Dimensions are summarized elsewhere.[22,23] Closely approximating C_{2h} symmetry, the cluster is composed of two $[Fe_4S_4]^0$ cubane cores (**5**) directly linked via two Fe−S bonds. The ensuing Fe_2S_2 rhomb is strictly planar, featuring Fe−Fe = 2.681(8) Å, Fe−S = 2.309(7) Å, and S−Fe−S = 110.7(2)°, consistent with the tetrahedral FeS_4 coordination of its iron atoms. Despite the change in core oxidation state, the mean Fe−P bond distance (2.412(6) Å) of the six tetrahedral sites **1** is not significantly different from that observed in $[Fe_4S_4(PCy_3)_4]^{1+}$ (2.40(3) Å). In conformity with the core structure, the Mössbauer spectrum consists of three overlapping quadrupole doublets (Figure 3). The spectrum was fit (without intensity constraints) to three doublets with the parameters in Table 4. The intensity-weighted isomer shift $\delta = 0.55$ mm/s is higher than the values for $[Fe_4S_4(PR_3)_4]^{1+}$, as would be expected for a fully reduced core. While rhombic M_2Q_2 interactions between clusters are frequently

(24) (a) Laskowski, E. J.; Frankel, R. B.; Gillum, W. O.; Papaethymiou, G. C.; Renaud, J.; Ibers, J. A.; Holm, R. H. *J. Am. Chem. Soc*. **1978**, *100*, 5322. (b) Laskowski, E. J.; Reynolds, J. G.; Frankel, R. B.; Foner, S.; Papaefthymiou, G. C.; Holm, R. H. *J. Am. Chem. Soc*. **1979**, *101*, 6562. (c) Carney, M. J.; Papaefthymiou, G. C.; Whitener, M. A.; Spartalian, K.; Frankel, R. B.; Holm, R. H. *Inorg. Chem*. **1988**, *27*, 346. (d) Carney, M. J.; Papaefthymiou, G. C.; Frankel, R. B.; Holm, R. H. *Inorg. Chem*. **1989**, *28*, 1497. Note that the isomer shifts in certain of these works are converted to values relative to Fe metal at room temperature by addition of 0.12 mm/s.

(25) Cambray, J.; Lane, R. W.; Wedd, A. G.; Johnson, R. W.; Holm, R. H. *Inorg. Chem*. **1977**, *16*, 2565.

(26) Pickett, C. J. *J. Chem. Soc., Chem. Commun*. **1985**, 323.

(27) (a) Agresti, A.; Bacci, M.; Cecconi, F.; Ghilardi, C.; Midollini, S. *Inorg. Chem*. **1985**, *24*, 689. (b) Cecconi, F.; Ghilardi, C.; Midollini, S.; Orlandini, A. *J. Chem. Soc., Dalton Trans*. **1987**, 831.

(28) Goddard, C. A.; Long, J. R.; Holm, R. H. *Inorg. Chem*. In press.

(29) (a) Fenske, D.; Ohmer, J.; Hachgenei, J. *Angew. Chem., Int. Ed. Engl*. **1985**, *24*, 993. (b) Fenske, D.; Ohmer, J.; Hachgenei, J.; Merzweiler, K. *Angew. Chem., Int. Ed. Engl*. **1988**, *27*, 1277.

(30) Steigerwald, M. D.; Siegrist, T.; Gyorgy, E. M.; Hessen, B.; Kwon, Y.-U.; Tanzler, S. M. *Inorg. Chem*. **1994**, *33*, 3389.

(31) In this context, we note the stable compounds $[Fe_4Te_4(PEt_3)_4]^{1+,0}$.[30,32,33] The mean Fe−P bond lengths of $[Fe_4Te_4(PR_3)_4]$ correlate with cone angle: R = Et (2.390(6) Å) < Pr^i (2.447(6) Å),[31b] as in the series $[Fe_4S_4(PR_3)_4]^{1+}$ above.

(32) Cecconi, F.; Ghilardi, C. A.; Midollini, S.; Orlandini, *J. Chem. Soc., Chem. Commun*. **1992**, 910.

(33) Steigerwald, M. D.; Siegrist, T.; Stuczynski, S. M.; Kwon, Y.-U. *J. Am. Chem. Soc*. **1992**, *114*, 3155.

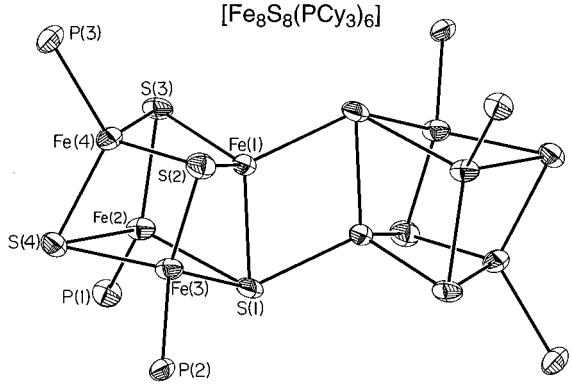

Figure 7. Core structure with phosphorus atoms (50% probability ellipsoids) and atom labeling scheme of the dicubane cluster $[Fe_8S_8(PCy_3)_6]$. The cluster resides on an inversion center. Selected intercubane interatomic distances (Å) and angles (deg): Fe−Fe 2.681(8), Fe−S 2.309(7), μ_4-S−Fe−μ_4-S 110.7(2). Selected mean intracubane interatomic distances (Å) and angles (deg) Fe−Fe 2.64(6), Fe−μ_4-S 2.38(2), Fe−μ_3-S 2.29(2), Fe−P 2.39(6), S−Fe−S 107(3), S−Fe−P 112(7), Fe−S−Fe 70(3).

observed in metal chalcogenide solid phases,[34] they are uncommon in molecular clusters.[35,36] In one example,[36] the dicubane formed by an Fe_2S_2 rhomb bridging two $MoFe_3S_4$ units is analogous to $[Fe_8S_8(PCy_3)_6]$.

Cubic Cluster: $[Fe_8S_6(PCy_3)_4Cl_4]$. Exploration of the reaction chemistry of the dicubane $[Fe_8S_8(PCy_3)_6]$, currently in progress, is hampered by the insolubility of the compound in all common solvents. However, $[Fe_8S_8(PCy_3)_6]$, when slurried in chloroform, immediately dissolves with reaction to form a dark brown solution. The same result is obtained with 1 equiv of SCl_2 in THF. Removal of solvent and dissolution of the residue in THF affords the compound $[Fe_8S_6(PCy_3)_4Cl_4]\cdot 3THF$ in modest yield (17%) upon slow crystallization. Its structure, set out in Figure 8, consists of an $[Fe_8S_6]^{4+}$ core built up of an idealized Fe_8 cube which is face-capped by six sulfide atoms. The cluster has imposed D_{2d} symmetry, requiring the adjacent iron atoms to have different terminal ligands. All iron sites have the tetrahedral configuration **1**, which we now associate with cone angles exceeding that of PEt_3.[20] Dimensional data are summarized in Table 5. The cubic cores $[Fe_8S_6]^{4+,5+}$ have been previously encountered in $[Fe_8S_6I_8]^{4-,3-}$, which were obtained in moderate yield after long or multiple recrystallization procedures.[37] We have no information on the means of formation of $[Fe_8S_6(PCy_3)_4Cl_4]$, but observe that phosphine has again contributed to the stabilization of an all-ferrous core.

Tetracubane Clusters: $[Fe_{16}S_{16}(PR_3)_8]$ (R = Bu^t, Pr^i). The self-assembly system $[FeCl_2(PEt_3)_2]/2NaSPh/4(PhCH_2S)_2S/6PPr^i_3$ in toluene was directed at the formation of the dicubane $[Fe_8S_8(PPr^i_3)_6]$. However, upon slow recrystallization of the reaction residue from acetonitrile, the product was obtained as black plates of $[Fe_{16}S_{16}(PPr^i_3)_8]\cdot 2MeCN$; multiple preparations gave yields below *ca*. 20%. In another approach, a solution of $[Fe_4S_4(PBu^t_3)_4]$ in benzene was layered with hexane and allowed to stand for 3 days. Black crystals of $[Fe_{16}S_{16}(PBu^t_3)_8]\cdot 2C_6H_{14}\cdot C_6H_6$ were obtained in 27% yield. Both compounds were identified by X-ray structure determinations.

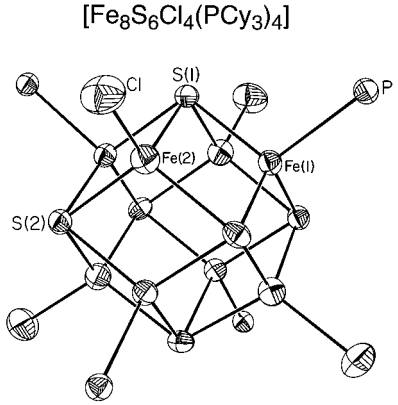

Figure 8. Core structure with chlorine and phosphorus atoms (40% probability ellipsoids) and atom labeling scheme of $[Fe_8S_6(PCy_3)_4Cl_4]$. The cluster resides on a $\bar{4}$ symmetry site with the rotation axis penetrating S(I).

Table 5. Selected Interatomic Distances (Å) and Angles (deg) for $[Fe_8S_6Cl_4(PCy_3)_4]$

Fe(1)−S(1)	2.272(3)	S(1)−Fe(2)−S(2″)	105.7(1)
Fe(1)−S(2′)	2.288(4)	S(2)−Fe(2)−S(1)	105.8(1)
Fe(1)−S(2″)	2.292(5)	S(2)−Fe(2)−S(2″)	108.9(1)
Fe(2)−S(1)	2.338(3)	Fe(1)−S(1)−Fe(2)	72.5(1)
Fe(2)−S(2)	2.323(5)	Fe(1′)−S(2)−Fe(2)	72.5(1)
Fe(2)−S(2″)	2.338(5)	Fe(1′)−S(2)−Fe(2‴)	69.5(1)
Fe(1)−Fe(2)	2.727(4)	Fe(1‴)−S(2)−Fe(2)	69.7(1)
Fe(1)−Fe(2′)	2.727(4)	Fe(1‴)−S(2)−Fe(2‴)	72.2(2)
Fe(1)−Fe(2″)	2.638(3)	S(1)−Fe(1)−P	107.7(2)
Fe(1)−P	2.422(5)	S(2′)−Fe(1)−P	109.2(2)
Fe(2)−Cl	2.219(6)	S(2″)−Fe(1)−P	109.4(2)
		Cl−Fe(2)−S(1)	115.0(2)
S(1)−Fe(1)−S(2′)	109.2(1)	Cl−Fe(2)−S(2)	110.7(2)
S(1)−Fe(1)−S(2″)	109.5(1)	Cl−Fe(2)−S(2″)	110.4(2)
S(2′)−Fe(1)−S(2″)	111.8(1)		

Because the detailed structures of the two clusters are insignificantly different, only that of $[Fe_{16}S_{16}(PBu^t_3)_8]$ is considered. The structure is depicted in Figure 9; selected interatomic distances and angles are listed in Table 6. It is immediately evident that the cluster is a *cyclic tetracubane*, a new structural motif in Fe−S cluster chemistry. The cluster has imposed D_4 symmetry; consequently, it is chiral. In geometric detail, the tetracubane cluster cores differ markedly from the dicubane core structure described above (see legend in Figure 7). The mean deviation of the atoms in the Fe_2S_2 intercubane rhombs of $[Fe_{16}S_{16}(PBu^t_3)_8]$ from a least-squares fitted plane is 0.08 Å, with the two Fe atoms pinched in toward the center of the cluster. Other dimensions are unexceptional.

As $[Fe_8S_8(PCy_3)_6]$, the two $[Fe_{16}S_{16}(PR_3)_8]$ clusters are highly insoluble in all common solvents. Thus far, we have been unsuccessful in obtaining di- and tetracubanes with the same phosphine. Apparently, the cluster isolated is that with the most favorable rate of crystallization, and it is formed by aggregation of single cubanes with concomitant loss of phosphine and generation of Fe_2S_2 intercubane rhombs. Four such rhombs are required in a cyclic tetracubane. The formation of three of these rhombs is rather easily visualized. The final step can be conceived as the folding of the incompletely cyclized tetracubane by pairwise coalescence of phosphorus and sulfur atoms. In practical terms, this is just the loss of two phosphine ligands and formation of the final two intercubane Fe−S bonds.

(34) For a recent example in Re−S/Se cluster chemistry, *cf*.: Long, J. R.; McCarty, L. S.; Holm, R. H. *J. Am. Chem. Soc*. **1996**, *118*, 4603 and references therein.

(35) Cubane-type $M_2M'_6S_8$ clusters (M = Co, Ni, Cu, Pd; M′ = Mo, W): (a) Shibahara, T.; Akashi, H.; Kuroya, H. *J. Am. Chem. Soc*. **1988**, *110*, 3313. (b) Shibahara, T.; Akashi, H.; Yamasaki, M.; Hashimoto, K. *Chem. Lett*. **1991**, 669. (c) Murata, T.; Mizobe, Y.; Gao, H.; Ishii, Y.; Wakabayashi, T.; Nakano, F.; Tanase, T.; Yano, S.; Hidai, M.; Echizen, I.; Nanikawa, H.; Motomura, S. *J. Am. Chem. Soc*. **1994**, *116*, 3389. (d) Shibahara, T.; Yamamoto, T.; Sakane, G. *Chem. Lett*. **1994**, 1221. See also: (e) $[Co_{12}(\mu_3\text{-}S)_{14}(\mu_4\text{-}S)_2(PEt_3)_{10}]^{2+}$: Cecconi, F.; Ghilardi, C. A.; Midollini, S.; Orlandini, A. *Inorg. Chim. Acta* **1993**, *214*, 13.

(36) $[Mo_2Fe_6(\mu_3\text{-}S)_6(\mu_4\text{-}S)_2(PEt_3)_6(O_2C_6Cl_4)_2]$: Demadis, K. D.; Campana, C. F.; Coucouvanis, D. *J. Am. Chem. Soc*. **1995**, *117*, 7832.

(37) (a) Pohl, S.; Saak, W. *Angew. Chem., Int. Ed. Engl*. **1984**, *23*, 907. (b) Pohl, S.; Opitz, U. *Angew. Chem., Int. Ed. Engl*. **1993**, *32*, 863.

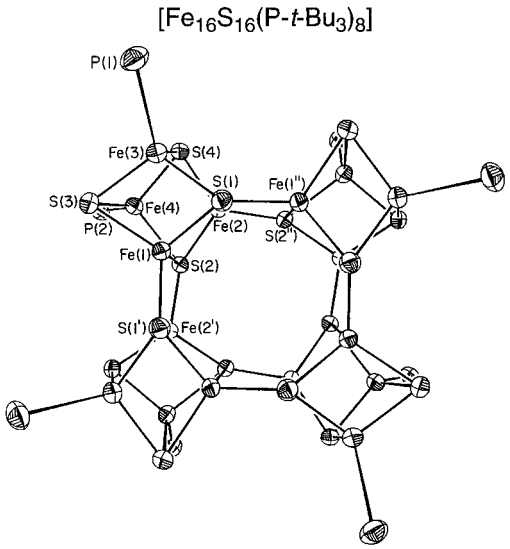

Figure 9. Core structure with phosphorus atoms (50% probability ellipsoids) and atom labeling scheme for one enantiomer of the tetracubane cluster $[Fe_{16}S_{16}(PBu^t_3)_8]$. View is down a crystallographically imposed four-fold rotation axis.

Table 6. Selected Interatomic Distances (Å) and Angles (deg) for $[Fe_{16}S_{16}(P^tBu_3)_8]\cdot 2C_6H_{14}\cdot C_6H_6$

Fe(1)−S(1′)	2.314(2)	Fe(1)−Fe(2)	2.527(1)
Fe(2)−S(2″)	2.287(2)		
mean of 2	2.30(1)	Fe(1)−Fe(3)	2.774(1)
		Fe(1)−Fe(4)	2.672(1)
Fe(1)−S(1)	2.345(2)	Fe(2)−Fe(3)	2.752(1)
Fe(1)−S(2)	2.382(2)	Fe(2)−Fe(4)	2.675(1)
Fe(2)−S(1)	2.367(2)	Fe(3)−Fe(4)	2.724(1)
Fe(2)−S(2)	2.345(2)	mean of 5	2.72(4)
Fe(3)−S(1)	2.383(2)		
Fe(4)−S(2)	2.360(2)	Fe(3)−P(1)	2.414(2)
mean of 6	2.36(2)	Fe(4)−P(2)	2.457(2)
		mean of 2	2.44(2)
Fe(1)−S(3)	2.323(2)		
Fe(2)−S(4)	2.320(2)		
mean of 2	2.322(2)		
		S(1′)−Fe(1)−S(2)	105.33(6)
Fe(3)−S(4)	2.277(2)	S(2″)−Fe(2)−S(1)	106.70(6)
Fe(3)−S(3)	2.283(2)		
Fe(4)−S(3)	2.296(2)	S(1′)−Fe(1)−S(1)	108.99(8)
Fe(4)−S(4)	2.299(2)	S(2″)−Fe(2)−S(2)	106.93(8)
mean of 4	2.289(9)		
		S(1′)−Fe(1)−S(3)	120.62(6)
Fe(1)−Fe(2′)	2.795(1)	S(2″)−Fe(2)−S(4)	120.32(6)
S(1)−Fe(1)−S(2)	112.86(6)	Fe(1″)−S(1)−Fe(2)	73.32(5)
S(2)−Fe(2)−S(1)	113.41(6)	Fe(2′)−S(2)−Fe(1)	73.52(5)
S(3)−Fe(1)−S(1)	103.01(6)	Fe(1″)−S(1)−Fe(1)	124.31(8)
S(3)−Fe(1)−S(2)	106.24(6)	Fe(2′)−S(2)−Fe(2)	124.97(8)
S(4)−Fe(2)−S(2)	105.74(6)		
S(4)−Fe(2)−S(1)	103.99(6)	Fe(1″)−S(1)−Fe(3)	126.33(7)
S(4)−Fe(3)−S(3)	105.91(7)	Fe(2′)−S(2)−Fe(4)	125.65(7)
S(4)−Fe(3)−S(1)	104.81(6)		
S(3)−Fe(3)−S(1)	103.03(6)	Fe(1)−S(1)−Fe(2)	64.86(5)
S(3)−Fe(4)−S(4)	104.77(6)	Fe(2)−S(2)−Fe(1)	64.62(5)
S(3)−Fe(4)−S(2)	107.86(6)		
S(4)−Fe(4)−S(2)	105.93(6)	Fe(1)−S(1)−Fe(3)	71.84(5)
		Fe(2)−S(1)−Fe(3)	70.83(5)
S(1)−Fe(3)−P(1)	107.30(7)	Fe(2)−S(2)−Fe(4)	69.31(5)
S(3)−Fe(3)−P(1)	115.10(7)	Fe(4)−S(2)−Fe(1)	68.60(5)
S(4)−Fe(3)−P(1)	119.08(7)	Fe(3)−S(3)−Fe(1)	74.06(5)
S(2)−Fe(4)−P(2)	104.42(6)	Fe(3)−S(3)−Fe(4)	73.00(5)
S(3)−Fe(4)−P(2)	120.99(7)	Fe(4)−S(3)−Fe(1)	70.69(5)
S(4)−Fe(4)−P(2)	111.97(7)	Fe(3)−S(4)−Fe(2)	73.54(5)
		Fe(3)−S(4)−Fe(4)	73.05(6)
		Fe(4)−S(4)−Fe(2)	70.78(5)

The Polycubane Cluster Family. The di- and tetracubane clusters $[Fe_8S_8(PCy_3)_6]$ and $[Fe_{16}S_{16}(PR_3)_8]$ (R = Bu^t, Pr^i) described above represent initial members in a potentially extensive family of polycubane clusters with formulae $[Fe_{4n}S_{4n}(PR_3)_p]$.[38] Given the possibility that other polycubanes may be sought experimentally, we offer a simple set of structural principles governing clusters in this family that may be extrapolated from just these two examples and some general attributes common to the majority of known iron−sulfur clusters. A polycubane cluster consists of an aggregate of n $[Fe_4S_4]^0$ cubane cores directly linked via $(4n - p)/2$ rhombic Fe_2S_2 interactions of the type displayed in $[Fe_8S_8(PCy_3)_6]$ (Figure 7). Each iron and each sulfur atom may partake in no more than one such linkage, and a total of p terminal phosphine ligands complete the tetrahedral coordination environment about those iron atoms which do not. Thus, all iron sites are tetrahedral and of two possible types: FeS_4 (as for Fe(1) in Figure 7) or FeS_3P (as for Fe(2,3,4)). Similarly, two different sulfur atom environments are possible: μ_4-S (with the geometry of S(1) in Figure 7) or μ_3-S (with the geometry of S(2,3,4)). While it is sterically feasible for a sulfur atom to partake in more than one rhombic Fe_2S_2 linkage, the particular μ_5-S entity required to form such an arrangement is entirely without precedent in iron−sulfur cluster chemistry, and the possibility is excluded on this basis.

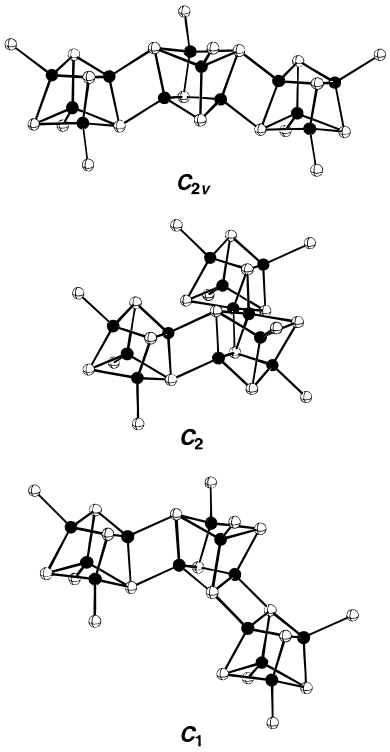

Figure 10. Core structures of the three distinct tricubane clusters; all have formula $[Fe_{12}S_{12}(PR_3)_8]$.

The foregoing rules delimit a family of structures that rapidly gains in complexity with increasing cubane aggregation number, n. Formally, the process of fusing two ideal monocubane clusters (**5**) into a single dicubane cluster entails coalescing a terminal L (=P) atom from each cubane with a μ_3-S atom in the other to form the two μ_4-S atom members of an Fe_2S_2 rhomb. For a single cubane there are twelve possible combinations of L and S atoms which may be employed for this purpose; however, given the T_d symmetry of the cluster, all twelve are equivalent. Thus, there is only one distinct dicubane cluster: $[Fe_8S_8(PR_3)_6]$, possessing the structure displayed in Figure 7. Enumeration of higher n-cubanes may be accomplished by

(38) The treatment which follows may, of course, be further generalized to polycubanes of formulae $[M_{4n}Q_{4n}L_p]$.

fusing a single cubane with each of the distinct $(n-1)$-cubanes in all possible manners, and eliminating duplicate structures.[39] Because each sulfur atom may participate in no more than one rhombic linkage, there are just fourteen different combinations of L and μ_3-S atoms in the dicubane cluster that may be used in attaching another cubane. Further, its C_{2h} symmetry dictates that only four of these fourteen combinations are distinct. Upon completing the fusion, two of the four ensuing structures are identical, leaving just the three distinct tricubane clusters, all of formula $[Fe_{12}S_{12}(PR_3)_8]$, displayed in Figure 10.[40] As of yet, there is no experimental evidence for the existence of any of these tricubane clusters, although the middle (C_2) structure (but not the other two) could conceivably precede formation of the tetracubane clusters $[Fe_{16}S_{16}(PR_3)_8]$ (R = Bu^t, Pr^i) in solution. Application of the fusion procedure to each of the tricubane structures generates a total of twenty distinct tetracubane structures.[40] Complete enumeration of polycubanes with $n \geq 5$ would necessitate a rigorous computer-implementation of this algorithm, as well as consideration of the steric complications which duly arise and the aforementioned flexibility associated with these structures.

The experimentally realized polycubane clusters adopt structures (Figures 7 and 9) in which every cubane core displays an identical coordination environment, an attribute common to other molecular and extended cluster assemblies.[41] None of the tricubane structures (Figure 10) possess this quality. Indeed, aside from the dicubane cluster, the only other "ideal" molecular polycubane (i.e., in which the core-linking Fe_2S_2 rhombs are strictly planar) that does is a cyclic $[Fe_{24}S_{24}(PR_3)_{12}]$ hexacubane cluster of S_6 symmetry formed by extending the linking geometry of the C_1 tricubane. Note that its empirical formula matches that of the observed tetracubanes. Quite possibly, the poor solubility of tetra- and pentacubane intermediates would prohibit formation of a hexacubane cluster. Also bearing the same empirical formula is the simple one-dimensional chain $[Fe_4S_4(PR_3)_2]$ formed by extending the C_{2v} tricubane such that each cubane core is linked to *two* neighboring cores through opposite coplanar Fe_2S_2 rhombs. A two-dimensional sheet structure, $[Fe_4S_4(PR_3)]$, wherein all cores are linked to *three* neighbors in an equivalent manner, is obtained from a hexagonal tiling using the S_6 hexacubane motif. Under the above-stated structural principles for polycubanes, there are two different ways in which a cubane core may be linked to the maximum of *four* neighboring cores. Representing each cubane core by a sphere situated at its center of mass, Figure 11 illustrates the disparate geometries of these two constructs. The upper geometry is compatible with the C_{2v}, and C_2 tricubane structures (Figure 10), while the lower geometry is compatible with the C_2 and C_1 tricubanes. Neither geometry is consistent with a commensurate two- or three-dimensional lattice. Thus, it is not possible to form an extended polycubane structure of formula $[Fe_4S_4]$ consisting solely of ideal, rhomb-linked cubane cores, each with an identical environment.

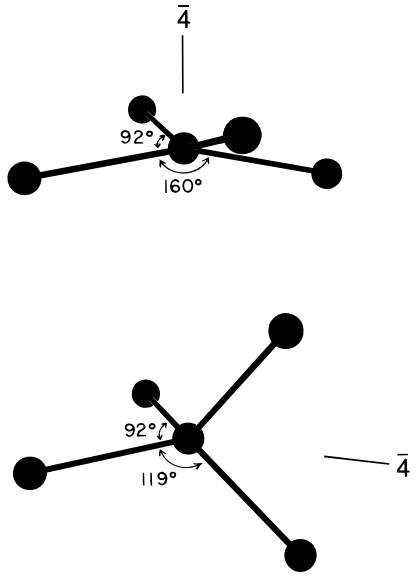

Figure 11. The two different possible geometries for an ideal $[Fe_4S_4]$ cubane core linked to four neighboring cores via strictly planar Fe_2S_2 rhombs. Cubane cores have been replaced with black spheres, whose centers lie 4.98 Å apart when the Fe−S distance is fixed at 2.26 Å. As such, the top geometry is a tetrahedron that has been *compressed* along the indicated $\bar{4}$ axis, and the bottom geometry is a tetrahedron that has been *elongated* along the indicated $\bar{4}$ axis.

Summary. The following are the principal results and conclusions of this investigation.

1. Reaction of the substitutionally labile cluster $[Fe_4S_4Cl_4]^{2-}$ with a small excess of PR_3 (R = Cy, Bu^t, Pr^i) in acetonitrile/THF results in the formation of $[Fe_4S_4(PR_3)_4]^{1+}$ whose $[Fe_4S_4]^{1+}$ core is one-electron more reduced than that of the starting cluster. These clusters have a cubane-type stereochemistry with standard dimensions and $S = {}^1/_2$ ground states with $g_{av} = 2.00$.

2. The clusters in (1) are the central members of the three-member electron transfer series $[Fe_4S_4(PR_3)_4]^{2+/1+/0}$. Attempts to isolate $[Fe_4S_4(PR_3)_4]^{2+}$ were unsuccessful. Chemical reduction of monocation clusters afforded $[Fe_4S_4(PR_3)_4]$ *in situ*, whose formation was demonstrated by mass spectrometry.

3. The clusters $[Fe_4S_4(PR_3)_4]$ upon standing in solution aggregate to form the dicubane or tetracubane clusters $[Fe_8S_8(PCy_3)_6]$ and $[Fe_{16}S_{16}(PBu^t_8)]$, respectively. $[Fe_8S_8(PCy_3)_6]$ and $[Fe_{16}S_{16}(PPr^i_8)]$ were prepared in self-assembly reaction systems which may first generate neutral monocubane clusters.

4. Formation of the polycubanes in (3) from neutral clusters involves the dissociation of PR_3 and formation of intercubane Fe−S bonds and Fe_2S_2 rhombs which link cubanes. The dicubane $[Fe_8S_8(PCy_3)_6]$ has only one structural precedent; $[Fe_{16}S_{16}(PR_3)_8]$ clusters (R = Bu^t, Pr^i) manifest cyclic tetracubane stereochemistry, a new structural motif in Fe−S cluster chemistry.

5. Tertiary phosphines exert two important properties in (1)−(4). (i) These ligands greatly stabilize the reduced $[Fe_4S_4]^{1+/0}$ oxidation states relative to conventional $[Fe_4S_4L_4]^{3-/4-}$ clusters (L = RS$^-$ and other monoanionic ligands). In particular, the $[Fe_4S_4]^0$ state has never been isolated in any other $[Fe_4S_4L_4]^z$ cluster. (ii) Ligands with cone angles in excess of that of PEt_3 (132°) stabilize tetrahedral FeS_3P sites (**1**) and thus cubane-type structures, whereas PEt_3 leads to the formation of (notably stable) basket ($[Fe_6S_6(PEt_3)_4L_2]$, $[Fe_6S_6(PEt_3)_6]^{1+}$) and face-capped octahedral ($[Fe_6S_8(PEt_3)_6]^{2+,1+}$) clusters which have trigonal pyramidal (**2**) and square-pyramidal iron sites, respectively. Fixedness of the all-ferrous $[Fe_4S_4]^0$ core appears to render the sulfide atoms sufficiently nucleophilic to engage in

(39) Owing to the multitude of possible connection pathways, the enumeration of polycubanes reduces to a nontrivial problem in graph theory, a field in which enumeration of even the simplest lattice-bound graphs relies upon such brutish iterative techniques: (a) Soteros, C. E.; Whittington, S. G. *J. Math. Chem.* **1990**, *5*, 307. (b) Long, J. R.; Holm, R. H. *J. Am. Chem. Soc.* **1994**, *116*, 9987.

(40) Only one enantiomer is counted (and displayed) for chiral polycubanes.

(41) To our knowledge, there are no relevant examples of cluster assemblies in which chemically identical cluster cores adopt more than one coordination environment. However, frameworks composed of two different cluster cores have been uncovered among the Chevrel phases: (a) Chevrel, R.; Sergent, M.; Seeber, B.; Fischer, Ø.; Grüttner, A.; Yvon, K. *Mater. Res. Bull.* **1979**, *14*, 567. (b) Chevrel, R.; Potel, M.; Sergent, M.; Decroux, M.; Fischer, Ø. *J. Solid State Chem.* **1980**, *34*, 247.

the formation of the two μ_4-S bridge sites present in each Fe_2S_2 rhomb which connects cubane cores in polycubanes.

6. A brief treatment of polycubane enumeration is presented, leading to predictions of possible stable structures for the smaller polycubanes with tetrahedral iron sites and planar Fe_2S_2 rhombs. Further considerations demonstrate that it is not possible to form an extended polycubane structure consisting of geometrically ideal, rhomb-linked $[Fe_4S_4]$ units, each with an identical environment.

The results of this investigation are currently being employed in the chemistry of higher nuclearity Fe−S clusters directed toward synthesis of the metal clusters in nitrogenase.[1]

Acknowledgment. This work was funded by NIH Grant GM 28856. We thank Dr. Lisheng Cai for experimental assistance, Professor E. Jacobsen for use of a susceptibility balance, and Dr. A. Tyler and Ms. J. Lynch for useful discussions and experimental assistance in mass spectrometry. X-ray diffraction equipment was obtained by NIH Grant 1 S10 RR 02247. The mass spectrometry facility at Harvard University is funded by NSF Grant CHE 9020043 and NIH Grant STO RR06716.

Supporting Information Available: X-ray structural information for the compounds in Tables 1 and 2, including tables of crystal and intensity collection data, positional and thermal parameters, and interatomic distances and angles (74 pages). See any current masthead page for ordering and Internet access instructions.

JA9620200